# Summertime subtropical sea surface temperature variability

A. M. Chiodi[1] and D. E. Harrison[1,2]

Received 31 August 2005; revised 15 February 2006; accepted 20 February 2006; published 19 April 2006.

[1] This paper describes a new class of summertime subtropical sea surface temperature (SST) anomalies that have basin scale, amplitudes up to 3°C and duration of up to 2 weeks. These have been discovered in the Microwave Imager (TMI) SST analyses. One-dimensional physics and numerical weather prediction operational air-sea fluxes are able to reproduce many aspects of the observations. The mechanism of creation of these summertime anomalies depends on the formation of shallow ocean mixed layer depths. Their persistence is controlled primarily by the duration of appropriate atmospheric conditions. Model studies also suggest that near synoptic scale surface flux variations, of the type considered here, cause significant warming of SST over monthly to seasonal timescales.
**Citation:** Chiodi, A. M., and D. E. Harrison (2006), Summertime subtropical sea surface temperature variability, *Geophys. Res. Lett.*, *33*, L08601, doi:10.1029/2005GL024524.

## 1. Introduction

[2] A novel class of basin scale, summertime, subtropical SST anomalies is described. The SST anomalies last from days to weeks and consist of increases up to 3°C from starting daily average SST, followed by decreases in SST of similar magnitude. Here, we describe the character of these newly found, summertime SST anomalies and their relation to the low wind conditions that drive them. Operational air-sea fluxes and a simple numerical one-dimensional ocean model are able to recreate many aspects of the observed anomalies.

[3] The anomalies were discovered in SST measurements obtained from the Microwave Imager (TMI) aboard the Tropical Rainfall Measuring Mission satellite. The unique look at SST that TMI provides has been instrumental in the discovery of other important processes that occur over several days to weeks [e.g., *Chelton et al.*, 2000; *Harrison and Vecchi*, 2001]. TMI samples virtually all of the ocean's surface between 40°S to 40°N within 2 to 3 days, even in the presence of clouds. TMI SST is thereby able to almost completely resolve the synoptic scale variability of the ocean. This timescale has not been well resolved before, because of the problem of cloud cover in traditional infrared-based satellite SST measurements [cf. *Wentz et al.*, 2000].

[4] The organization of this paper is as follows. Section 2 describes the data and one-dimensional mixed layer model used herein. Section 3 presents examples of the summertime SST events from observations and modeling. Section 4 discusses implications of the SST variability presented here.

## 2. Data and Methods

[5] Since December of 1997, TMI has measured SST at $0.25° \times 0.25°$ resolution with an estimated accuracy of 0.5°C in rain-free conditions [*Wentz et al.*, 2000]. The daily ascending and descending tracks (v3a, available from Remote Sensing Systems at www.ssmi.com) are first linearly filled in time and then the time-filled ascending and descending track data are averaged onto a 1° grid. Submonthly variability is isolated by high-pass filtering, accomplished here by subtracting 30-day boxcar smoothed data from 7-day boxcar smoothed data.

[6] Observed SST is compared to the SST estimated from a classic numerical ocean mixed layer model. The model is driven with daily mean surface fluxes of heat, momentum and moisture obtained from the National Centers for Environmental Prediction (NCEP) reanalysis of global atmospheric fields and surface fluxes [*Kalnay et al.*, 1996]. The daily mean surface fluxes are linearly interpolated to the model time step, so the diurnal cycle is unresolved in both the fluxes and model. Shortwave radiation is assumed to consist of two wavelengths that are attenuated vertically with 0.6m and 20m e-folding scales. The model (PWP), chosen for its conceptual simplicity, applies heat and moisture fluxes to the water column and entrains water into the mixed layer when wind stress drives vertical shear above a critical bulk Richardson number or when the density profile becomes unstable [*Price et al.*, 1986]. Parameters are standard with vertical resolution set at 1 m in order to resolve the very shallow (2–5 m) mixed layer depths. A background diffusion of $2 \times 10^{-5}$ $m^2/s$ is applied uniformly throughout the water column. The SST predicted from this model has been shown to be remarkably similar to other, more complex, mixed layer models [*Large and Crawford*, 1995; *Shinoda and Hendon*, 1998].

[7] To illustrate the surface atmospheric conditions typically associated with the warming events, a composite average of ten events has been made. The events occur in various locations which prevents using a fixed geographic frame of reference for the composite. Instead, we use the location of the peak SST as the origin of the composite grid. The latitude and longitude on this grid refers to distance away from the observed peaks of high-passed SST (see Figure 1). Once interpolated to the composite grid, NCEP sea level pressure (SLP), wind speed and TMI SST from the ten events were averaged according to days before or after the peak SST, i.e., composite day-1 represents the composite average 1 day before the peak SST occurs. Northern hemisphere events are composited with north and south reversed so that they match the southern

[1]Joint Institute for the Study of the Atmosphere and the Ocean, University of Washington, Seattle, Washington, USA.
[2]NOAA Pacific Marine Environmental Laboratory, Seattle, Washington, USA.


0094-8276/06/2005GL024524$05.00

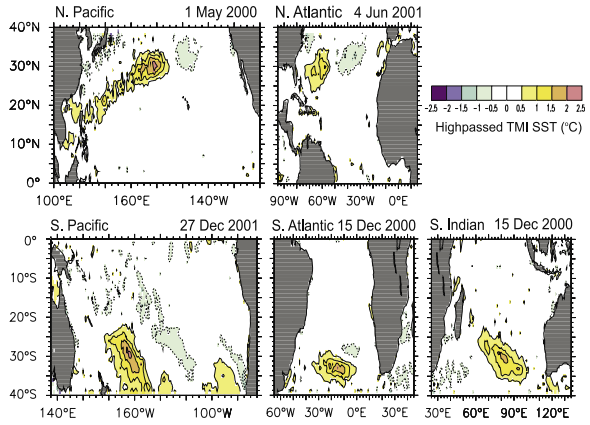


**Figure 1.** Snapshots of high-passed SST events.

hemisphere geostrophic frame of reference chosen for the composite.

## 3. Results

[8] Basin-scale, coherent regions of high-passed SST above 0.5°C have been observed in each subtropical ocean basin (e.g., Figure 1). High-passed SST above 0.5°C indicates rapid warming, followed by rapid cooling of the SST over the course of several days to weeks. The high-passed SST patterns are typically slanted such that their western flanks extend equatorward of the eastern portions and tend to be centered at approximately ±30° of latitude, near the reversal from trades to westerly winds.

[9] Hovmöller diagrams have shown that several warming events occur in each late spring to early summer season, whereas high-pass SST during the rest of the year, in a given basin, fails to show phenomena at the 1° to 2°C level. Events grow in place at various longitudes. Multiple events are usually seen in a given year, each usually lasting about a week or two. A single basin is shown here for figure clarity (Figure 2). The other subtropical ocean basins show similar seasonality.

[10] A composite average of 10 warming events was made to illustrate the near surface atmospheric conditions typically associated with the events (Figure 3). It is evident that low wind speed conditions (thick contours in Figure 3) appear about a week before the SST maxima occurs. The calm conditions are associated with a newly forming high pressure system (thin contours in Figure 3), which peaks about the time the SST maxima occurs. The peak SST is reached as the anticyclone associated with the high pressure system begins to break up or move. As winds return to normal levels, SST cools nearly as rapidly as it had warmed.

[11] Moist anomalies of 0.8–1.2 g/kg were also observed in composites of 2m height specific humidity (not shown) in the days leading up to the peak SST. Along with light winds, this moisture anomaly accounted for a reduction in latent heat loss of 40–50 W/m$^2$ from the climatological average, during these days, and also accounted for a 5–10% reduction in net surface radiative heat loss.

[12] The evolution of the warming events is explained by 1-D physics and daily mean to weekly surface flux variability. In the formation stage, large downward heatflux stratifies the original ocean mixed layer because wind mixing is lower than normal. The new shallow mixed layer (top few meters depth) then warms abruptly, for multiple days, until wind speed increases. When winds increase, downward heat flux decreases and wind mixing entrains water below the mixed layer. The mixed layer then deepens and cools over the next several days.

[13] When integrated in a numerical ocean mixed layer model, daily mean NCEP surface fluxes reproduce many aspects of the observed SST. A year of model and observed SST, spatially averaged over 174°E to 180° and 29°N to 30°N, is shown in the inset of Figure 4a. The North Pacific

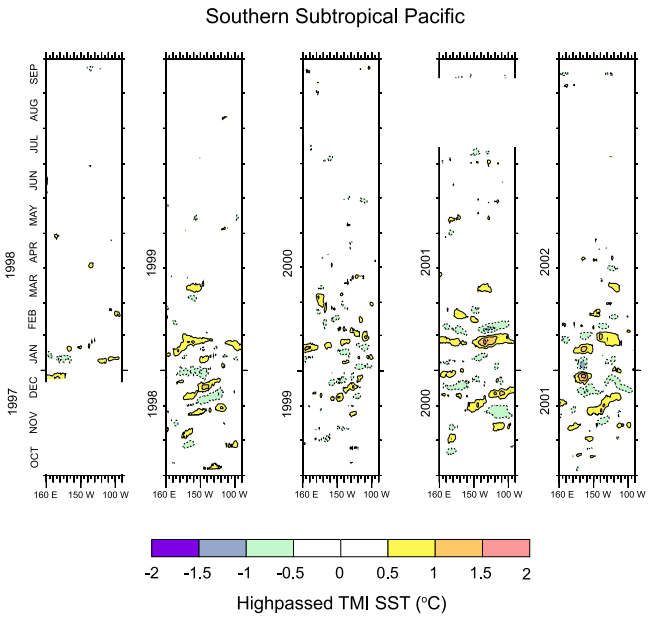


**Figure 2.** Hovmöller diagram of 27°S–33°S average high-passed TMI SST.

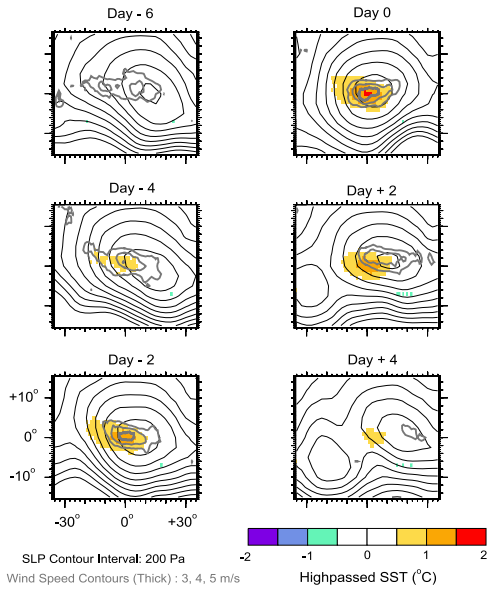


**Figure 3.** TMI SST (color field), NCEP SLP (thin black lines) and wind speed (thick gray lines) composited from 10 SST warming events.

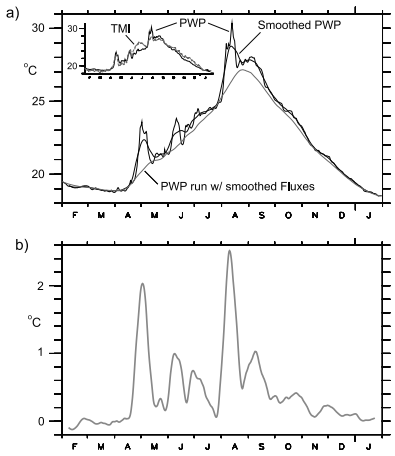


**Figure 4.** (a) PWP model SST from integration of 174°E–180°, 29°N-30°N area average, daily mean NCEP surface fluxes (thin black curve). This same model SST, smoothed with a 30-day boxcar filter (thick black curve). PWP SST resulting from integration of surface fluxes which are first smoothed with a 30-day boxcar filter (gray curve). (inset) Initial model SST (solid curve) and TMI SST (dashed curve). (b) Difference between the smoothed initial model SST, and the SST resulting from integration of the smoothed fluxes.

event captured in Figure 1 appears here as the 3–4 degree spike in TMI SST (dashed line) that peaks on 1 May 2000. Other warming events with a 1–2-week timescale can be seen at the beginning of June and August. The SST resulting from integration of daily average fluxes (solid line in inset and thin curve in Figure 4a) accurately reproduces the timing and amplitude of the May and June warming events. The amplitude of the August event is over-predicted by the model, although the timing of the event is well reproduced. A discrepancy between the model and TMI SST occurs in early July. This difference may be due to errors in fluxes or horizontal advection, which is not accounted for in the model. Overall, the close resemblance of the model and TMI SST in Figure 4 shows that both the high frequency components, and seasonal cycle of SST is reproduced accurately with this simple model of mixed layer processes, and standard surface flux products.

[14] To investigate the importance of synoptic scale surface flux variability on SST, synoptic scale variations were eliminated from the daily mean surface fluxes by applying a 30-day boxcar filter to the fluxes prior to a second integration. The 30-day boxcar filter was applied to the magnitude of the wind stress vector which was then decomposed into zonal and meridional components according to daily mean wind direction. This was done so that filtration caused no change in net momentum flux. The direction of the wind has little importance in this integration. The SST resulting from integrating the boxcar filtered fluxes (thick gray curve, Figure 4a) was then compared to the 30-day boxcar filtered original model SST (thick black curve, Figure 4a).

[15] The warming events do not appear in the SST resulting from integration of the filtered fluxes, which was observed to be several °C lower than the original model SST during event peaks (Figure 4b). Interestingly, the difference between the two models remains above zero after the warming events. A residual warming of a few tenths °C remains throughout fall despite the lack of warming events in September and October. This result suggests that, in addition to the abrupt warming that occurs during the events themselves, the rectified warming of synoptic scale fluctuations in momentum and heat flux may play an important role in seasonal subtropical SST anomalies.

## 4. Summary and Discussion

[16] Using microwave SST data, we have discovered that basin scale, multi-day SST warming events, up to 3°C in magnitude, are common features of the summertime subtropics. This abrupt warming of SST occurs over large, coherent spatial scales (approximately 2500 km) commensurate with the atmospheric phenomena that drive them. A simple one-dimensional mixed layer model, integrated with daily mean reanalysis surface fluxes, accurately reproduces the timing, and often, magnitude of the warming events. This implies that the reanalysis fluxes contain fairly accurate synoptic scale variability over broad regions of the subtropics, especially with regard to wind-driven variations. This finding is in agreement with point-wise comparison of the reanalysis fluxes with tropical, in situ measurements [cf. *Shinoda and Hendon*, 1998; *Bernie et al.*, 2005; *Anderson et al.*, 1996].

[17] It is well known that the diurnal SST cycle can have magnitudes of 1°C or more when insolation is strong and winds are light. Diurnal cycles of ≈1°C have been described in the tropical Pacific [*Anderson et al.*, 1996] and Indian Oceans [*Shinoda and Hendon*, 1998; *Bernie et al.*, 2005]. Case studies have revealed larger cycles in the subtropics [e.g., *Flament et al.*, 1994; *Stramma et al.*, 1986]. Infrared based satellite data has been used to characterize diurnal cycling [*Cornillon and Stramma*, 1985; *Tanahashi et al.*, 2003; *Stuart-Menteth et al.*, 2003] and diurnal cycling, observed in TMI SST, has been described by *Gentemann et al.* [2003].

[18] The SST anomalies described and successfully modeled here appear to depend on longer-than-diurnal cycle forcing. It is not possible to investigate the extent to which including diurnal forcing would alter the model results presented here because the operational fluxes cannot provide the hourly time resolution that is needed to investigate the diurnal cycle. That the results presented here track the observations as well as they do when only daily average forcing is used suggests strongly that diurnal aspects are of at most secondary importance. There is an observational feature that also supports this view; the peak SST during the Northern Pacific event shown in Figure 1 was measured at 2315 local time. All the measurements several days prior to and after the peak SST were also at night. If the low wind/high insolation physics that have been shown to produce a substantial diurnal cycle in SST [e.g., *Bernie et al.*, 2005; *Shinoda*, 2005] were the cause of this SST anomaly, a several °C peak in SST would not be observed near local midnight.

[19] The nearly degree-per-day warming and 200–250 W/m$^2$ daily mean net heat flux that occur during the events imply that mixed layer depths are shallow (<5 m),

perhaps even 1–2 m, depending on the degree of shortwave attenuation in the mixed layer. This suggests that, in order for ocean models to reproduce the observed SST variability, the vertical resolution of the model, in and near the mixed layer, must be on the order of 1 m or less. Shallow mixed layer depths occur in the model during the events; the model shown in Figure 4 attains average mixed layer depths of 1.7 and 2.7 m, respectively, during the warming events that took place during 25–30 April and 5–10 June 2000.

[20] The synoptic time scale forcing contained in the daily average NCEP fluxes satisfactorily reproduces the multi-day SST events described here. Otherwise, identical experiments forced with a 30-day running average filtered version of the daily mean forcing do not reproduce the total amount of observed surface warming either during the period when multi-day warming events occur (Figure 4b, April through August mean inter-model SST difference $\approx$0.5°C) or over the several subsequent months (Figure 4b, September through November). The multi-day SST warming events depend upon the formation of a shallow mixed layer which is not formed when the filtered forcing is applied. The subsequent persistence of warm SST results from a rectified wind-forced response, because the mixed layer depth and net surface heat flux co-vary (stronger wind increases cooling from latent heat flux and also produces a a deeper mixed layer, and vice versa). Awareness of a higher-frequency, insolation-forced version of this type of rectification has been discussed in studies of diurnal SST and mixed layer variability [cf. *Shinoda and Hendon*, 1998; *Bernie et al.*, 2005; *Shinoda*, 2005].

[21] It is notable that both the SST events described here and synoptic scale atmospheric anticyclones are more often seen poleward of 20° latitude [see *Jones and Simmonds*, 1994; *Sinclair*, 1996]. This suggests that the tendency for atmospheric anticyclones to remain in the subtropics to mid-latitudes is what keeps the SST events from consistently occurring in the tropics.

[22] Any feedback effects that SST warming events have on the atmospheric phenomena which create them may be important since anticyclones have been determined to be instrumental in the development of low-level atmospheric bands of easterlies and westerlies [*Kuo*, 1951]. The fact that SST, and therefore the lower boundary condition to the atmosphere, evolves on the spatial and timescales of the anticyclones, possibly, provides motivation for future study.

[23] **Acknowledgments.** AMC would like to acknowledge helpful conversations with J. M. Wallace and use of TMI processing methods developed by G. A. Vecchi. PMEL contribution 2856.

## References

Anderson, S. P., R. A. Weller, and R. B. Lukas (1996), Surface buoyancy forcing and the mixed layer of the western Pacific warm pool: Observations and 1D model results, *J. Clim.*, *9*, 3056–3085.

Bernie, D. J., S. J. Woolnough, J. M. Slingo, and E. Guilyardi (2005), Modeling diurnal intraseasonal variability of the ocean mixed layer, *J. Clim.*, *18*, 1190–1202.

Chelton, D. B., F. J. Wentz, C. L. Gentemann, R. A. de Szoeke, and M. G. Schlax (2000), Satellite microwave SST observations of transequatorial tropical instability waves, *Geophys. Res. Lett.*, *9*, 1239–1242.

Cornillon, P., and L. Stramma (1985), The distribution of diurnal sea surface warming events in the western Sargasso Sea, *J. Geophys. Res.*, *90*, 11,811–11,815.

Flament, P., J. Firing, M. Sawyer, and C. Trefois (1994), Amplitude and horizontal structure of a large diurnal seas surface warming event during the coastal ocean dynamics experiment, *J. Phys. Oceanogr.*, *24*, 124–139.

Gentemann, C., C. J. Donlon, A. Stuart-Menteth, and F. J. Wentz (2003), Diurnal signals in satellite sea surface temperature measurements, *Geophys. Res. Lett.*, *30*(3), 1140, doi:10.1029/2002GL016291.

Harrison, D. E., and G. A. Vecchi (2001), January 1999 Indian Ocean cooling event, *Geophys. Res. Lett.*, *28*, 3717–3720.

Jones, D. A., and I. Simmonds (1994), A climatology of southern hemisphere anticyclones, *Clim. Dyn.*, *10*, 333–348.

Kalnay, E., et al. (1996), The NCEP/NCAR 40-year reanalysis project, *Bull. Am. Meteorol. Soc.*, *77*, 437–471.

Kuo, H.-L. (1951), Vorticity transfer as related to the development of the general circulation, *J. Meteorol.*, *8*, 307–315.

Large, W. G., and G. B. Crawford (1995), Observation and simulations of upper-ocean response to wind events during the ocean storms experiment, *J. Phys. Oceanogr.*, *25*, 2831–2852.

Price, J. F., R. A. Weller, and R. Pinkel (1986), Diurnal cycling: Observations on models of the upper ocean response to diurnal heating, cooling and wind mixing, *J. Geophys. Res.*, *91*, 8411–8427.

Shinoda, T. (2005), Impact of the diurnal cycle of solar radiation on intraseasonal SST variability in the western equatorial Pacific, *J. Clim.*, *18*, 2628–2636.

Shinoda, T., and H. H. Hendon (1998), Mixed layer modeling of intraseasonal variability in the tropical western Pacific and Indian Ocean, *J. Clim.*, *11*, 2668–2685.

Sinclair, M. R. (1996), A climatology of anticyclones and blocking for the Southern Hemisphere, *Mon. Weather Rev.*, *124*, 245–263.

Stramma, L., P. Cornillon, R. A. Weller, J. F. Price, and M. G. Briscoe (1986), Large diurnal sea surface temperature variability: Satellite and in situ measurements, *J. Phys. Oceanogr.*, *16*, 827–837.

Stuart-Menteth, A. C., I. S. Robinson, and P. G. Challenor (2003), A global study of diurnal warming using satellite-derived sea surface temperature, *J. Geophys. Res.*, *108*(C5), 3155, doi:10.1029/2002JC001534.

Tanahashi, S., H. Kawamura, T. Takahashi, and H. Yusa (2003), Diurnal variations of sea surface temperature over the wide-ranging ocean using VISSR on board GMS, *J. Geophys. Res.*, *108*(C7), 3216, doi:10.1029/2002JC001313.

Wentz, F. J., C. L. Gentemann, D. Smith, and D. Chelton (2000), Satellite measurements of sea surface temperature through clouds, *Science*, *288*, 847–850.

A. M. Chiodi and D. E. Harrison, Joint Institute for the Study of the Atmosphere and the Ocean, University of Washington, Box 355351, Seattle, WA 98195–5351, USA. (chiodi@ocean.washington.edu)